JCTC Journal of Chemical Theory and Computation

Assessment of Functionals for TD-DFT Calculations of Singlet−Triplet Transitions

Denis Jacquemin,*[,†] Eric A. Perpète,[†] Ilaria Ciofini,[‡] and Carlo Adamo*[,‡]

Groupe de Chimie-Physique Théorique et Structurale, Facultés Universitaires Notre-Dame de la Paix, Rue de Bruxelles, 61, B-5000 Namur, Belgium, and Ecole Nationale Supérieure de Chimie de Paris, Laboratoire Electrochimie et Chimie Analytique, UMR CNRS-ENSCP no. 7575, 11, Rue Pierre et Marie Curie, F-75321 Paris Cedex 05, France

Received January 4, 2010

Abstract: The calculation of transition energies for electronically excited states remains a challenge in quantum chemistry, for which time-dependent density functional theory (TD-DFT) is often viewed as a balanced (computational effort/obtained accuracy) technique. In this study, we benchmark 34 DFT functionals in the specific framework of TD-DFT calculations for singlet−triplet transitions. The results are compared to accurate wave function data reported for the same set of 63 excited-states, and it turns out that, within the selected TD-DFT framework, BMK and M06−2X emerge as the most efficient hybrids. This investigation clearly illustrates that the conclusions drawn for singlet excited states do not necessarily hold for triplet states, even for similar molecular structures.

1. Introduction

Time-dependent density functional theory (TD-DFT)[1−7] is probably the most extensively used theoretical tool for the computing electronic transition energies in organic or inorganic compounds. In the recent years, a series of benchmark calculations aimed at appraising the relative qualities of DFT functionals in the TD-DFT framework have appeared.[8−12] Although the detailed conclusions might significantly differ from one work to the other (e.g., see the discussion in ref 12), the typical mean absolute deviation (MAE) obtained with the most efficient functionals is in the range of 0.20−0.30 eV for singlet excited states. In the present article, we aim at evaluating the *pros* and *cons* of an extended panel of functionals for the calculation of singlet−triplet transitions, as the number of previous benchmarks remains limited, despite several specific TD-DFT applications for these states.[13−17] On the one hand, Grimme and Neese compared the B3LYP and double-hybrid singlet−triplet energies for a series of small molecules,[18] for which they obtained an average deviation limited to 0.25 eV with B3LYP and 0.18 eV with B2PLYP. On the other hand, Thiel and co-workers used their high-level ab initio estimates for 63 singlet−triplet transitions to assess the efficiency of TD-DFT calculations relying on the BP86, B3LYP, BHHLYP functionals as well as the DFT/multireference−configuration interaction (DFT/MR-CI) procedure.[10] The average deviations range from 0.4 to 0.6 eV for the three functionals, significantly exceeding the errors observed for the singlet−singlet transition energies in the same molecules. This is in full agreement with other works, hinting that the results produced with TD-DFT could be less accurate and significantly more functional-dependent for triplet states than for singlet states.[15,19]

One should note that the results presented in this contribution have been obtained by "traditional" TD-DFT, requiring extreme care when considering spin-flipping transitions if the target open-shell excited state cannot be described with a single-determinant model. Specific models have been developed to overcome such difficulties.[20,21] In this framework, it is worth pinpointing the investigation by Nguyen and co-workers who computed the $S_0 - T_1$ energy difference, for a large set of organic molecules, using UB3LYP calculations.[22] The results appeared pretty accurate, at the

* Corresponding authors. E-mail: denis.jacquemin@fundp.ac.be (D.J.) and carlo-adamo@enscp.fr (C.A.).

† FUNDP, Namur.

‡ ENSCP, Paris.

10.1021/ct100005d
Published on Web 04/14/2010

price of the limitation of the computational procedure to the lowest-lying triplet.

In this article, we investigate the efficiency of more than 30 DFT functionals within the TD-DFT formalism, considering the same set of transitions as in ref 10 as references. Therefore, we assess the functional's qualities using accurate wave function estimates, rather than experimental values. This choice is motivated, on the one hand, by the intention to ensure perfectly meaningful comparisons and, on the other hand, by the comparatively (with respect to the singlet case) limited number of accurate experimental data available in literature.

2. Method

As benchmark set, we have selected the list of singlet−triplet transitions recently gathered together by Thiel's group.[10,23] This set includes 20 small- and medium-sized compounds and a total of 63 excited states that have been treated with CAS-PT2, CC2, and CC3, theoretical best estimates have also been determined. For the transitions under scrutiny in this letter, these best estimates generally correspond to the CC3 values. All calculations reported here have been performed with the Gaussian suite of programs, with a tight self-consistent field convergence threshold (10^{-8}−10^{-10} au), using both commercial and development versions.[24−26] The MP2/6-31G(d) geometries were recovered from ref 23, and the eight-to-twenty first vertical triplet excited states have been computed with TD-DFT/TZVP. As demonstrated in Section 4, in which EOM-CCSD and TD-DFT calculations are performed with larger basis sets [6-311+G(2d,p), 6-311++G(3df,3pd), and aug-cc-pVTZ], several transition energies are significantly altered by including diffuse functions, but the statistical impact of using larger basis sets remains limited.

As we assess the performances of DFT approaches, we have selected a large panel of functionals, including local density approximation (LDA), generalized gradient approximation (GGA), meta-GGA, global hybrids (GH), and range-separated hybrids (RSH): SVWN5, BLYP, BP86, OLYP, PBE, M06-L, VSCX, τ-HCTCH, TPSS, TPSSh, O3LYP, τ-HCTCH-hyb, B3LYP, B3P86, X3LYP, B98, PBE0, mPW1PW91, M06, M05, BMK, BHHLYP, M06-2X, M05-2X, M06-HF, LC-ωPBE (20), LC-BLYP, LC-OLYP, LC-PBE, LC-τHCTH, LC-TPSS, LC-ωPBE, and CAM-B3LYP. We have also included the CIS approach for comparison purposes. We refer the reader to ref 12 for appropriate bibliographic informations for these functionals.

3. Results and Discussion

The transition energies obtained for all molecules and functionals as well as statistical analysis are catalogued in the Supporting Information. For the extensive benchmark calculations presented here, it is probably useless to discuss the computed spectra molecule-per-molecule, as such specific analysis is already available for three typical functionals in ref 10. Consequently, we will focus here on global results, allowing to unravel general trends, thanks to statistical analysis.

Table 1. Statistical Analysis for the Full Set of Transitions, Using the Theoretical Best Estimates As References[a]

functional	MSE	MAE	SD	rms	*b*	R^2
CIS	0.12	0.56	0.37	0.67	1.11	0.82
SVWN5	0.35	0.42	0.37	0.56	0.95	0.88
BLYP	0.48	0.49	0.33	0.58	0.96	0.93
BP86	0.49	0.49	0.32	0.58	0.97	0.93
OLYP	0.46	0.46	0.32	0.50	0.97	0.93
PBE	0.50	0.50	0.33	0.60	0.96	0.93
M06-L	0.37	0.38	0.24	0.45	0.98	0.96
VSXC	0.43	0.43	0.25	0.49	0.98	0.96
τ-HCTH	0.55	0.55	0.25	0.61	0.98	0.96
TPSS	0.49	0.49	0.26	0.55	0.98	0.96
TPSSh	0.51	0.51	0.23	0.55	0.98	0.97
O3LYP	0.43	0.43	0.22	0.49	0.98	0.97
τ-HCTH-hyb	0.42	0.42	0.20	0.46	0.99	0.97
B3LYP	0.44	0.44	0.19	0.48	0.99	0.98
B3P86	0.45	0.45	0.19	0.49	0.99	0.98
X3LYP	0.44	0.44	0.19	0.48	0.99	0.98
B98	0.37	0.37	0.20	0.42	1.00	0.98
PBE0	0.49	0.49	0.21	0.54	0.99	0.97
mPW1PW91	0.51	0.51	0.22	0.55	0.99	0.97
M06	0.44	0.44	0.18	0.47	0.99	0.98
M05	0.70	0.70	0.34	0.78	0.98	0.95
BMK	0.18	0.24	0.16	0.28	0.99	0.97
BHHLYP	0.54	0.58	0.46	0.73	0.95	0.90
M06-2X	0.07	0.23	0.17	0.28	0.98	0.94
M05-2X	0.22	0.27	0.20	0.33	0.98	0.96
M06-HF	−0.06	0.44	0.26	0.51	1.02	0.87
LC-ωPBE (20)	0.45	0.45	0.21	0.49	1.00	0.97
LC-BLYP	0.34	0.36	0.19	0.41	1.05	0.97
LC-OLYP	0.32	0.35	0.20	0.40	1.06	0.97
LC-PBE	0.37	0.40	0.21	0.44	1.08	0.97
LC-τ-HCTH	0.49	0.50	0.31	0.58	1.08	0.95
LC-TPSS	0.39	0.42	0.25	0.49	1.10	0.97
LC-ωPBE	0.50	0.55	0.38	0.66	1.17	0.93
CAM-B3LYP	0.41	0.42	0.24	0.48	1.05	0.97

[a] MSE is the mean signed error (reference-TD-DFT), MAE is the mean absolute error, SD is the standard deviation, and RMS is the residual mean squared error. MSE, MAE, SD, and RMS are in eV, and *b* and R^2 are the slope and the squared correlation coefficient, respectively, obtained through an unconstrained least-square linear fit.

The computed mean signed error (MSE), MAE, standard deviation (SD), root-mean-square deviation (rms) as well as the slope (*b*) and R^2 determined by unconstrained linear fittings that can be found in Table 1, whereas Figure 1 provides error profiles for a selection of functionals (VSXC, PBE0, M06-2X, and CAM-B3LYP). In the Supporting Information, the reader will find tables with MSE, MAE, rms, and R^2, using CAS-PT2 or CC3 values as benchmarks rather than the "best theoretical estimates". While the average errors and correlation coefficients differ from the results listed in Table 1, the discrepancies remain limited to a typical ±0.04 eV for the MSE, MAE, and rms and ±0.02 for the R^2. The similarities between the CAS-PT2 and CC3 transition energies are clear in ref 10, and we consequently only use the "best estimates" as reference values in the following, except when explicitly noted.

As can be seen in Table 1, the MSE values are systematically positive, but for M06-HF, that includes 100% of exact exchange, indicating that DFT functionals tend to almost systematically underestimate the transition energies. For the traditional GH, incorporating 20% and 30% of HF-like exchange, the errors are large (e.g., PBE0 in Figure 1) with typical deviations larger than 0.40 eV, except for B98 (0.37

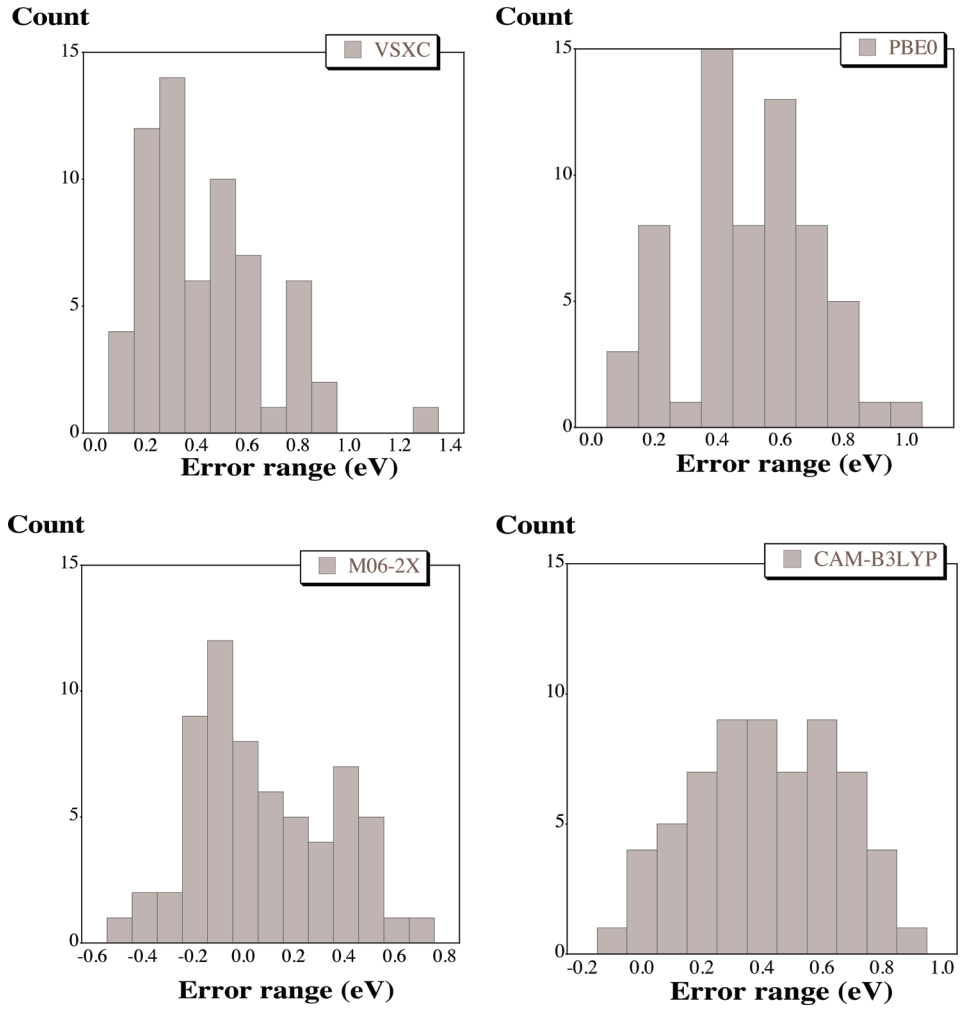

Figure 1. Histogram of the errors (eV) computed for four representative functionals.

eV). In fact, the M06-L meta-GGA outperforms most traditional hybrids on the MSE criterion. In the present case, the selection of range-separated methodologies does not help improve the estimates; the MSE values are systematically larger than 0.35 eV for the eight RSH functionals (see CAM-B3LYP histogram in Figure 1). It turns out that only four schemes yield |MSE| below the 0.2 eV threshold: BMK, M06-2X, M06-HF, and CIS. This finding strongly contrasts with singlet excited-states for which GH with 22−25% of exact exchange produces the smallest MSE.[12] The MAE delivered by most functionals are similar to that of the MSE, owing to the systematic overestimation effect. Only three theoretical schemes lead to average absolute errors smaller than 0.3 eV, namely: BMK (0.24), M06-2X (0.23), and M05-2X (0.27 eV). For the record, the more refined and computationally demanding DFT/MR-CI approach provides a similar MAE (0.25 eV) for the same set of molecules.[10] It is striking that the CIS scheme, characterized by a small MSE, yields the largest MAE, whereas the BHHLYP scheme produces much larger deviations (MAE of 0.58 eV) than functionals including a similar amount of exact exchange, like BMK or M06-2X. This indicates that the HF/DFT mixing is not the only major parameter governing the response of hybrids contrary to singlet−singlet transitions for which this parameter mostly guides the final answer. Such a statement is confirmed by comparing the B98/X3LYP and M06/M05 columns in the Supporting Information; the computed transition energies significantly differ though these functionals rely on very similar exact exchange ratios. In what concerns the consistency of the computed values, one notes that CIS provides the poorest agreement with the reference data ($R^2 = 0.82$). The SVWN5 LDA also yields a poor R^2 (0.88), while all GGA (meta-GGA) deliver correlation coefficients of 0.93 (0.96), clearly indicating that climbing Jacob's ladder of functionals improves the consistency of the results, although it might be detrimental for the average errors. Most tested GH values are characterized by large correlation coefficients (0.97−0.98) and by slopes reasonably close to 1. It is worth noting that the M06-2X R^2 of 0.94 increases to 0.96 when CAS-PT2 and CC3 reference data are selected. Nevertheless, BMK apparently grants slightly more consistent singlet−triplet energies than M06-2X. Eventually, we note that the R^2 of all RSH are similar to that of global hybrids, except for LC-ωPBE ($R^2 = 0.93$). This result is consistent with the larger damping parameter (0.40) used in LC-ωPBE; it delivers results almost identical to GH, including a large share of exact exchange. In short, this investigation clearly demonstrates that the optimal functionals within the TD-DFT framework significantly differ for singlet and triplet excited states. Indeed, for the latter, BMK (see Figure 2) and M06-2X emerge as the two most promising approaches, whereas the performance of BMK is

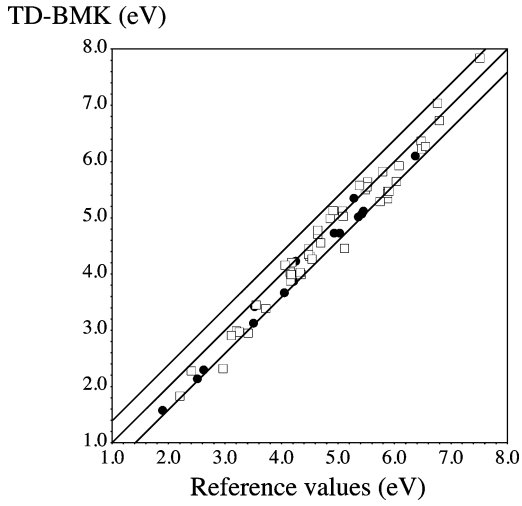

Figure 2. Comparisons between TD-BMK and theoretical best estimates (ref 10) for singlet−triplet transitions. The open squares (closed circles) correspond to $\pi \rightarrow \pi^\star$ ($n \rightarrow \pi^\star$) transitions. The central line indicates a perfect match, whereas the two side lines are border for ±0.4 eV deviations.

relatively modest for singlet states.[12] These two functionals provide a precision that is not far from that obtained with refined TD-DFT approaches including spin-flipping transitions,[27] as it has been shown that also in this case, large HF exchange contributions are needed to get accurate values. Therefore, it could be argued that the best-performing functionals, all containing a very large percent of HF exchange, could somehow handle such problems.

We have also performed a statistical analysis limited to the first singlet−triplet transition of each molecule, as TD-DFT is often viewed as particularly well-suited for describing low-lying states. For the present set of molecules, the R^2 improves for the majority of functionals, but no systematic decrease (wrt the full set) of the MAE or the rms is oberved. Indeed, the MAE computed for pure (RSH) functionals significantly decrease (increase) with relatively trifling variations for GH (but M05 and BHHLYP). For instance, as the BLYP MAE goes from 0.49 eV (full set) to 0.38 eV (first states), the B3LYP MAE changes by a negligible +0.01 eV, whereas the LC-BLYP MAE raises from 0.36 eV to 0.44 eV. In fact, the two most effective functionals remain BMK and M06-2X, with respective MAE of 0.26 and 0.20 eV. In the Supporting Information, tables specific to the $n \rightarrow \pi^\star$ and $\pi \rightarrow \pi^\star$ states are also given. For the first family of transitions, estimates are particularly sensitive to the actual form of the functional, as expected. For instance, the MAE of two meta-GGA, M06-L, and TPSS are similar (0.40 eV and 0.44 eV) for the full set but differ by more than 50% (0.37 eV and 0.63 eV) for $n \rightarrow \pi^\star$ transitions. For these states, a much larger correlation coefficient is obtained. Indeed, all hybrids (but BHHLYP) present a R^2 of 0.98 or 0.99 for the $n \rightarrow \pi^\star$ transitions. This is fully consistent with our previous works for singlet states.[12,28] Surprisingly, the BHHLYP MAE is minimal (0.21 eV), though BMK and M06-2X still perform satisfactorily (MAE of 0.27 and 0.26 eV, respectively, see also Figure 2). The most striking difference wrt the full set is probably the improved accuracy of RSH for $n \rightarrow \pi^\star$ excitations. The error patterns for $\pi \rightarrow \pi^\star$ are similar to that of the full set, with the M06−2X, BMK, and M05-2X leading to the smallest average deviations.

Table 2. Investigation of the Basis Set Effects for Three Typical Functionals[a]

		EOM-CCSD			CC3	
functional		TZVP	6-311+G (2d,p)	6-311++G (3df,3pd)	TZVP	BE
B3LYP	MSE	0.50	0.47	0.47	0.47	0.44
	MAE	0.50	0.47	0.47	0.47	0.44
	SD	0.22	0.18	0.18	0.18	0.19
	rms	0.54	0.50	0.50	0.51	0.48
	b	0.97	0.98	0.99	1.00	0.99
	R^2	0.97	0.98	0.98	0.98	0.98
M06-2X	MSE	0.13	0.13	0.13	0.11	0.07
	MAE	0.26	0.23	0.22	0.23	0.23
	SD	0.17	0.16	0.16	0.18	0.17
	rms	0.31	0.28	0.27	0.29	0.28
	b	0.97	0.98	0.99	1.00	0.99
	R^2	0.95	0.96	0.96	0.96	0.94
CAM-B3LYP	MSE	0.47	0.45	0.43	0.45	0.41
	MAE	0.47	0.45	0.43	0.45	0.42
	SD	0.18	0.18	0.18	0.24	0.24
	rms	0.50	0.48	0.47	0.51	0.48
	b	1.04	1.05	1.06	1.06	1.05
	R^2	0.98	0.98	0.98	0.97	0.97

[a] The same basis set is used for wavefunction and TD-DFT calculations. BE is the theoretical best estimates. See caption of Table 1 for more details.

4. Basis Set Effects

The results presented in Section 3 rely on the TZVP basis set for both the tested TD-DFT approaches and the wave function references. For sure, one expects that using larger diffuse-containing basis sets would induce significant variations of the computed transition energies, especially for the wave function schemes. For this reason, we have used Gaussian09 to perform EOM-CCSD calculations with three more extended basis sets, namely 6-311+G(2d,p), 6-311++G(3df,3pd), and aug-cc-pVTZ[29] (see Table 4 in the Supporting Information). This choice of EOM-CCSD as a reference method is justified because, according to Thiel,[23] all CC schemes behave well for singlet−triplet states. This statement is confirmed by Table 2 in which the statistical data collected using CC3/TZVP or EOM-CCSD/TZVP references are typically within 0.03 eV of each other.

As expected, using diffuse-containing basis sets tends to decrease the computed transition energies, though in most cases, the effect is relatively limited. Indeed, taking the aug-cc-pVTZ values as reference, we have computed EOM-CCSD mean absolute variation of 0.07, 0.02, and 0.01 eV for TZVP, 6-311+G(2d,p), and 6-311++G(3df,3pd), respectively (see Table 4 in the Supporting Information). Basically, 6-311+G(2d,p) provides converged EOM-CCSD results, and the largest deviation with respect to the aug-cc-pVTZ results is limited to −0.12 eV (A″ state of imidazole); the second largest discrepancy being as small as −0.06 eV (B_{2u} state of benzene). It is certainly appropriate to state that the EOM-CCSD/6-311++G(3df,3pd) energies are almost free of any basis set influence, at least for the transitions investigated herein. In Table 2, we perform a statistical analysis for three hybrid functionals using larger basis sets for both TD-DFT and wave function approaches. As can

be seen, using larger basis sets tends to slightly decrease the average errors of all three functionals, but this effect remains small and does not affect the relative performances of each functional, the variations being similar for the three hybrids. For instance the B3LYP, M06-2X and CAM-B3LYP MAE are 0.50, 0.26, and 0.47 eV, respectively, with TZVP and become 0.47, 0.22, and 0.43 eV with 6-311++G(3df,3pd). These minor variations originate in almost parallel evolution of the transition energies at the TD-DFT and EOM-CCSD levels. The states that are strongly basis set dependent (or unaffected by the size of the basis set) at the EOM-CCSD level are the same at the TD-DFT level. For instance, the sensitive (insensitive) A″ state of imidazole (B_2 state of pyrrole) varies by −0.74 eV (−0.04 eV) when shifting from TZVP to aug-cc-pVTZ at the EOM-CCSD level, while the shift is −0.76 (−0.03), −0.64 (−0.10), and −0.48 eV (−0.03 eV) at the B3LYP, M06−2X, and CAM-B3LYP levels, respectively.

5. Conclusions

Using the set of "best available" wave function values provided by Thiel, we have benchmarked more than 30 density functional theory (DFT) functionals in the framework of time-dependent density functional theory (TD-DFT) evaluations of singlet−triplet transition energies. It turned out that: (i) for most functionals, the average deviations are larger than for singlet excited states; (ii) hybrids relying on similar exact exchange proportion but with different exchange−correlation forms might deliver significantly different values, especially for $n \rightarrow \pi^\star$ transitions; (iii) BMK and M06-2X allow taking the inner track to accurate estimates with MAE close to 0.25 eV in all cases, whereas B3LYP and PBE0 deviations are typically larger than 0.40 eV; (iv) range-separated formalism yield large errors for $\pi \rightarrow \pi^\star$ transitions; (v) these noted trends hold for the lowest-lying states, whereas substantial differences between $n \rightarrow \pi^\star$ and $\pi \rightarrow \pi^\star$ have been unravelled; and (vi) though a few transition energies are strongly affected by basis set effects, these "statistical" conclusions pertain for larger basis sets.

We are currently considering larger molecules and experimental benchmarking of DFT functionals.

Acknowledgment. D.J. and E.A.P. thank the Belgian National Fund for Scientific Research for their research associate and senior research associate positions, respectively. The authors thank Prof. G.E. Scuseria for the use of LCH. G03 and G09 calculations have been performed on the Interuniversity Scientific Computing Facility (ISCF), installed at the Facultés Universitaires Notre-Dame de la Paix (Namur, Belgium), for which the authors gratefully acknowledge the financial support of the FNRS-FRFC and the "Loterie Nationale" for the convention number 2.4578.02 and of the FUNDP. The collaboration between the Belgian and French group is supported by the Wallonie-Bruxelles International, the Belgian Fonds de la Recherche Scientfique, the Ministere Français des Affaires étrangeres et européennes, and the Ministere de l'Enseignement supérieur et de la Recherche in the framework of Hubert Curien Partnership.

Supporting Information Available: Tables with all transition energies, statistical data, and basis set study. This material is available free of charge via the Internet at http://pubs.acs.org.

References

(1) Runge, E.; Gross, E. K. U. *Phys. Rev. Lett.* **1984**, *52*, 997–1000.

(2) Stratmann, R. E.; Scuseria, G. E.; Frisch, M. J. *J. Chem. Phys.* **1998**, *109*, 8218–8224.

(3) Casida, M. E. In *Time-dependent density-functional response theory for molecules*; Chong, D. P., Ed.; World Scientific: Singapore, 1995; Vol. 1, pp 155−192.

(4) Perdew, J. P.; Ruzsinsky, A.; Tao, J.; Staroverov, V. N.; Scuseria, G. E.; Csonka, G. I. *J. Chem. Phys.* **2005**, *123*, 062201.

(5) Dreuw, A.; Head-Gordon, M. *Chem. Rev.* **2005**, *105*, 4009–4037.

(6) Barone, V.; Polimeno, A. *Chem. Soc. Rev.* **2007**, *36*, 1724–1731.

(7) Jacquemin, D.; Perpète, E. A.; Ciofini, I.; Adamo, C. *Acc. Chem. Res.* **2009**, *42*, 326–334.

(8) Peach, M. J. G.; Benfield, P.; Helgaker, T.; Tozer, D. J. *J. Chem. Phys.* **2008**, *128*, 044118.

(9) Rohrdanz, M. A.; Herbert, J. M. *J. Chem. Phys.* **2008**, *129*, 034107.

(10) Silva-Junior, M. R.; Schreiber, M.; Sauer, S. P. A.; Thiel, W. *J. Chem. Phys.* **2008**, *129*, 104103.

(11) Goerigk, L.; Moellmann, J.; Grimme, S. *Phys. Chem. Chem. Phys.* **2009**, *11*, 4611–4620.

(12) Jacquemin, D.; Wathelet, V.; Perpete, E. A.; Adamo, C. *J. Chem. Theory Comput.* **2009**, *5*, 2420–2435.

(13) Paddon-Row, M. N.; Shephard, M. J. *J. Phys. Chem. A* **2002**, *106*, 2395–2944.

(14) Chong, D. P. *J. Electron Spectrosc. Relat. Phenom.* **2005**, *148*, 115–121.

(15) Santoro, F.; Improta, R.; Lami, A.; Bloino, J.; Barone, V. *J. Chem. Phys.* **2007**, *126*, 184102.

(16) Lanzo, I.; Russo, N.; Sicilia, E. *J. Phys. Chem. B* **2008**, *112*, 4123–4130.

(17) Caricato, M.; Trucks, G. W.; Frisch, M. J.; Wiberg, K. B. *J. Chem. Theory Comput.* **2010**, *6*, 370–383.

(18) Grimme, S.; Neese, F. *J. Chem. Phys.* **2007**, *127*, 154116.

(19) Tozer, D. J.; Handy, N. C. *Phys. Chem. Chem. Phys.* **2000**, *2*, 2117–2121.

(20) Shao, Y.; Head-Gordon, M.; Krylov, A. I. *J. Chem. Phys.* **2003**, *118*, 4807–4818.

(21) Wang, F.; Ziegler, T. *J. Chem. Phys.* **2004**, *121*, 12191–12196.

(22) Nguyen, K. A.; Kennel, J.; Pachter, R. *J. Chem. Phys.* **2002**, *117*, 7128–7136.

(23) Schreiber, M.; Silva-Junior, M. R.; Sauer, S. P. A.; Thiel, W. *J. Chem. Phys.* **2008**, *128*, 134110.

(24) Frisch, M. J.; Trucks, G. W.; Schlegel, H. B.; Scuseria, G. E.; Robb, M. A.; Cheeseman, J. R.; Montgomery, J. A., Jr.; Vreven, T.; Kudin, K. N.; Burant, J. C.; Millam, J. M.; Iyengar, S. S.; Tomasi, J.; Barone, V.; Mennucci, B.; Cossi, M.; Scalmani, G.; Rega, N.; Petersson, G. A.; Nakatsuji, H.; Hada, M.; Ehara, M.; Toyota, K.; Fukuda, R.; Hasegawa, J.;

Ishida, M.; Nakajima, T.; Honda, Y.; Kitao, O.; Nakai, H.; Klene, M.; Li, X.; Knox, J. E.; Hratchian, H. P.; Cross, J. B.; Bakken, V.; Adamo, C.; Jaramillo, J.; Gomperts, R.; Stratmann, R. E.; Yazyev, O.; Austin, A. J.; Cammi, R.; Pomelli, C.; Ochterski, J. W.; Ayala, P. Y.; Morokuma, K.; Voth, G. A.; Salvador, P.; Dannenberg, J. J.; Zakrzewski, V. G.; Dapprich, S.; Daniels, A. D.; Strain, M. C.; Farkas, O.; Malick, D. K.; Rabuck, A. D.; Raghavachari, K.; Foresman, J. B.; Ortiz, J. V.; Cui, Q.; Baboul, A. G.; Clifford, S.; Cioslowski, J.; Stefanov, B. B.; Liu, G.; Liashenko, A.; Piskorz, P.; Komaromi, I.; Martin, R. L.; Fox, D. J.; Keith, T.; Al-Laham, M. A.; Peng, C. Y.; Nanayakkara, A.; Challacombe, M.; Gill, P. M. W.; Johnson, B.; Chen, W.; Wong, M. W.; Gonzalez, C.; Pople, J. A. *Gaussian 03*, revisions D.02 and E.01, Gaussian, Inc.: Wallingford, CT, 2004.

(25) Gaussian DV, Revision G.01; Frisch, M. J.; Trucks, G. W.; Schlegel, H. B.; Scuseria, G. E.; Robb, M. A.; Cheeseman, J. R.; Scalmani, G.; Barone, V.; Mennucci, B.; Petersson, G. A.; Nakatsuji, H.; Caricato, M.; Li, X.; Hratchian, H. P.; Izmaylov, A. F.; Bloino, J.; Zheng, G.; Sonnenberg, J. L.; Hada, M.; Ehara, M.; Toyota, K.; Fukuda, R.; Hasegawa, J.; Ishida, M.; Nakajima, T.; Honda, Y.; Kitao, O.; Nakai, H.; Vreven, T.; Montgomery, Jr., J. A.; Peralta, J. E.; Ogliaro, F.; Bearpark, M.; Heyd, J. J.; Brothers, E.; Kudin, K. N.; Staroverov, V. N.; Kobayashi, R.; Normand, J.; Raghavachari, K.; Rendell, A.; Burant, J. C.; Iyengar, S. S.; Tomasi, J.; Cossi, M.; Rega, N.; Millam, N. J.; Klene, M.; Knox, J. E.; Cross, J. B.; Bakken, V.; Adamo, C.; Jaramillo, J.; Gomperts, R.; Stratmann, R. E.; Yazyev, O.; Austin, A. J.; Cammi, R.; Pomelli, C.; Ochterski, J. W.; Martin, R. L.; Morokuma, K.; Zakrzewski, V. G.; Voth, G. A.; Salvador, P.; Dannenberg, J. J.; Dapprich, S.; Daniels, A. D.; Farkas, Ö.; Foresman, J. B.; Ortiz, J. V.; Cioslowski, J.; Fox, D. J. Gaussian, Inc.: Wallingford, CT, 2009.

(26) Frisch, M. J.; Trucks, G. W.; Schlegel, H.s B.; Scuseria, G. E.; Robb, M. A.; Cheeseman, J. R.; Scalmani, G.; Barone, V.; Mennucci, B.; Petersson, G. A.; Nakatsuji, H.; Caricato, M.; Li, X.; Hratchian, H. P.; Izmaylov, A. F.; Bloino, J.; Zheng, G.; Sonnenberg, J. L.; Hada, M.; Ehara, M.; Toyota, K.; Fukuda, R.; Hasegawa, J.; Ishida, M.; Nakajima, T.; Honda, Y.; Kitao, O.; Nakai, H.; Vreven, T.; Montgomery, J. A., Jr.; Peralta, J. E.; Ogliaro, F.; Bearpark, M.; Heyd, J. J.; Brothers, E.; Kudin, K. N.; Staroverov, V. N.; Kobayashi, R.; Normand, J.; Raghavachari, K.; Rendell, A.; Burant, J. C.; Iyengar, S. S.; Tomasi, J.; Cossi, M.; Rega, N.; Millam, N. J.; Klene, M.; Knox, J. E.; Cross, J. B.; Bakken, V.; Adamo, C.; Jaramillo, J.; Gomperts, R.; Stratmann, R. E.; Yazyev, O.; Austin, A. J.; Cammi, R.; Pomelli, C.; Ochterski, J. W.; Martin, R. L.; Morokuma, K.; Zakrzewski, V. G.; Voth, G. A.; Salvador, P.; Dannenberg, J. J.; Dapprich, S.; Daniels, A. D.; Farkas, Ö.; Foresman, J. B.; Ortiz, J. V.; Cioslowski, J.; Fox, D. J. et al. *Gaussian 09* , revision A.2, Gaussian, Inc.: Wallingford, CT, 2009.

(27) Wang, F.; Ziegler, T. *J. Chem. Phys.* **2005**, *122*, 074109.

(28) Jacquemin, D.; Perpete, E. A.; Vydrov, O. A.; Scuseria, G. E.; Adamo, C. *J. Chem. Phys.* **2007**, *127*, 094102.

(29) For the latter basis sets, the two largest molecules (octatetraene and naphthalene) were beyond computational reach.

CT100005D